Functional shifts in natural forests under environmental change over the last 65 years are faster in colder regions

Masumi Hisano
Lakehead University https://orcid.org/0000-0002-3869-8542
Han Chen (hchen1@lakeheadu.ca)
Lakehead University https://orcid.org/0000-0001-9477-5541
Xinli Chen
Lakehead University https://orcid.org/0000-0003-0542-5959
Masahiro Ryo
Freie Universität Berlin https://orcid.org/0000-0002-5271-3446

Article

Keywords: Functional shifts, forest ecosystems, colder regions, ecosystem management practices

Posted Date: October 7th, 2020

DOI: https://doi.org/10.21203/rs.3.rs-85210/v1

Abstract

Global environmental changes have significantly impacted plant diversity and composition over many decades. Maintaining biodiversity and composition is critical for sustainability of ecosystem functioning and related services. While global environmental changes have modified plant species and functional compositions in forest ecosystems, it remains unclear how temporal shifts in functional composition differ across regions and biomes. Utilizing extensive spatial and long-term forest inventory data (17,107 plots monitored 1951–2016) across Canada, we found that functional composition shifted toward fast-growing deciduous broadleaved trees and higher drought tolerance over time; notably, this functional shift was more rapid in colder regions. Further analysis revealed that the functional composition of colder plots shifted toward drought tolerance more rapidly with rising CO2 than warmer plots, which suggests the vulnerability of the functional composition of colder plots against global environmental changes. Future ecosystem management practices should consider spatial differences in functional responses to global environmental change, with particular attention to colder plots that experience higher rates of warming and compositional changes.

Background

Global environmental change is altering terrestrial plant diversity and composition worldwide [1], and therefore, understanding how they react to the change through time is a central theme in ecology [2]. Rising atmospheric CO_2 favours fast-growing species [3,4], and increasing temperatures have caused directional shifts in plant species composition toward thermophilic [5] and resource acquisitive traits [6]. Additionally, more frequent droughts have increased the abundance of dry-affiliated plant taxa [4,7] by favouring the competitive ability of trees toward drought-tolerant strategies [8]. As these compositional changes can critically influence changes in forest biomass [9], which is an important measure of terrestrial carbon dynamics, understanding the long-term responses of functional composition can provide insights into the sustainability of global forest ecosystem functioning [10] and related services, and by extension, humanity [11]. However, our knowledge of temporal global environmental change-induced compositional shifts is limited to regional scales, or within the same biome that shares similar biogeographical and climatic influences. To aid in the development of globally applicable strategies for ‘climate action’ [12], it is imperative to quantify how rapidly compositional shifts occur on larger scales across biomes.

Canada has wide variations in its baseline climate (i.e., local historic climate), as both mean annual temperatures and precipitation can vary substantially (Figs. 1a, b). Eastern Canada possesses higher water availability than the central and western regions of the country, as it receives a greater quantity of the mean annual precipitation, which satisfies the mean annual evapotranspiration demand (Fig. 1a). Moreover, Canada experiences spatially diverse temporal climate driving trends. For example, temporal changes in water availability varied significantly between regions (Fig. 1c), although both atmospheric CO_2 concentrations and temperatures consistently rose across Canada, with higher warming rates at higher latitudes (Fig. 1d). At regional scales, spatial differences in the baseline climate have been shown

to affect the temporal trends of biomass changes in boreal forests. For example, the growth of boreal forests in colder regions that experienced lower, or no changes in water availability, were less negatively affected by long-term climate change compared to boreal forests in the warmer regions of Eastern Canada [13]. Moreover, boreal forests in more humid regions suffered a lower extent of biomass loss under long-term changes in climate in Western Canada [14]. If long-term global environmental change favours tree species with traits that are better adapted to new climate realities (while causing higher mortality for species with unfavoured traits), these differences in demographic changes may induce spatially divergent shifts in functional composition. However, exactly how temporal shifts in functional traits are associated with spatial gradients of the baseline climate have rarely been tested, with insights being limited only to a water availability gradient in tropical forests [7]. Yet, we are not cognizant of how the rate and directionality of compositional shifts are dependent on larger scale environmental contexts across regions and biomes, particularly as relates to baseline temperature. Moreover, no study as yet has determined the relative contributions of these regionally dependent environmental change drivers to shifts in functional composition of natural forests at a macroecological, cross-biome scale.

For this paper, we explored how the directionality and rate of temporal functional changes of natural forests in response to persistent long-term global environmental change have been dependent on baseline climatic conditions over 65 years across multiple biomes in Canada. We hypothesized that, overall, the compositions of forests across Canada would shift toward resource acquisitive deciduous broadleaved trees in response to rising CO_2 and temperatures [3,15]. Further, the functional composition of forests in drier plots would respond more quickly to long-term global environmental change than humid plots, by increasing community-level drought tolerance due to their greater susceptibility to decreasing water availability [14]. Moreover, the functional shifts of colder plots would be more prominent than their warmer plots due to the higher propensity for increased temperatures at higher latitudes [16] (Fig. 1). To test these hypotheses, we surveyed the data for 17,107 permanent sampling plots (with 1,471,165 trees naturally regenerated following wildfire and unmanaged) of temperate and boreal forests monitored between 1951 and 2016 across Canada (Fig. 1). We represented functional composition by the community-weighted mean (CWM) [17] of eight traits associated with competitive and tolerative abilities. These included leaf nitrogen and phosphorus content per leaf dry mass, specific leaf area, wood density, shade tolerance, drought tolerance [18], leaf habit, and leaf structure (Fig. 2). To compress the dimensionality, we used the first and second axes of the principal component analysis (PCA). The first axis was correlated with deciduous broadleaved trees vs. conifers (CWM_{PC1}, positively associated with leaf nitrogen and phosphorus content, specific leaf area, and wood density), whereas the second axis was negatively correlated with drought tolerance ($CWM_{PC2} \times -1$; converted to make it positively associated with drought tolerance; Fig. 2). Subsequently, we analyzed temporal trends in these functional composition metrics over 65 years (representing changes in atmospheric CO_2 concentration, temperature, and water availability), while simultaneously accounting for the influences of stand development [19] and spatial variations in the baseline climate (i.e., long-term averages of mean annual temperature (MAT_{ave}) and climate moisture index (CMI_{ave}) [13,14]. Further, we examined the relationships between functional

shifts and temporal trends in atmospheric CO_2 concentrations, anomalies of mean annual temperature (ATA), and the climate moisture index (ACMIA).

Results And Discussions

Across all study plots and temporally repeated measurements, stand age (0.2 to 379 years; succession following stand-replacing disturbances) accounted for more variations in both functional composition metrics, and it had greater effect sizes on them than background temporal changes (i.e., calendar year) (Fig. 3). Overall, the functional composition shifted toward conifers and lower drought tolerance (or higher shade tolerance; see Fig. 2) with stand age (Fig. 4a). Increased baseline water availability (CMI_{ave}) was the most strongly associated with conifers and lower drought tolerance (Fig. 4b), while baseline temperature (MAT_{ave}) showed the strongest association with deciduous broadleaved trees and lower drought tolerance (Fig. 4c).

Even after factoring out the potent influences of stand age and baseline climate covariates, we found that functional composition shifted toward deciduous broadleaved trees and higher drought tolerance (or lower shade tolerance) over the calendar year (see the main black lines in Fig. 5). This was consistent with a previous study of the boreal and temperate forests of Western Canada [15], Eastern USA [9], and Europe [29]. Furthermore, our analysis revealed that the functional shift toward drought tolerance over the calendar year was strongly modulated by baseline temperature (Fig. 5d), while the shift speed was nearly consistent regardless of water availability (Figs. 3, 5c). Specifically, drought tolerance increased (or shade tolerance decreased) with the calendar year more rapidly in colder plots than warmer plots (Fig. 5d), and even the slope direction was opposite in the case of warmer plots. The temporal shift toward deciduous broadleaved trees was consistent across the baseline climate (Figs. 3, 5a). To understand the functional shift process, we examined temporal changes in the relative abundance of major tree genera (Fig. S1). We found that the observed trends in functional composition, as related to the baseline temperature, were due to greater temporal increases in the relative abundance of deciduous broadleaved trees and early-successional conifers (particularly *Betula* and *Pinus*) with a reduction in drought intolerant conifers (*Picea*; see Table S2 for genus-level trait values) in colder plots (Fig. S1b). This suggested the higher sensitivity of functional composition in boreal forests at higher latitudes (Fig. 1b) under long-term global environmental change.

Over the 65 years, the atmospheric CO_2 concentrations (Fig. 1e) and temperature (ATA) increased across the study area (Figs. 1d, f, g). However, the temperature rose more quickly in wetter and colder sites, in contrast to drier and warmer sites (Figs. 1f, g). Across the study area, water availability (ACMIA) showed a convex curve, which increased and then decreased over the calendar year (Figs. 1f, g). However, drier sites experienced more substantial temporal variations in water availability, although the most humid sites exhibited a gradual concave curve, which decreased and then increased over the calendar year (Fig. 1f). The temporal trend in water availability was consistently concaved with the baseline temperature (Fig. S1g).

To investigate whether the expedited compositional shifts at colder sites were the result of more rapidly warming temperatures, we replaced the baseline climate variables in eqn. 1 with temporal change rates in temperature ($ATA_{ChangeRate}$) and water availability ($ACMIA_{ChangeRate}$) (Figs. 1c, d, S2). We found that the functional shift toward drought tolerance was more prominent in plots with higher change rates in temperature, $ATA_{ChangeRate,}$ than those in water availability (Fig. S3). Thus, the faster shifts in functional composition towards drought tolerance/shade intolerance in colder plots were likely due to more rapid warming than the change in water availability in those plots (Figs. 1b, g).

We then tested whether the association of functional composition with these global environmental change drivers would be dependent on the baseline climate. We employed two alternative approaches (one driver at a time, and all three drivers simultaneously, using a linear mixed-effect model, respectively) to model the main and interactive effects of individual drivers and baseline climate on functional composition. These approaches yielded similar coefficient estimates (Fig. S4). As interpreted from the results of the linear mixed models with all three drivers modelled simultaneously, CO_2 had the greatest effect size on both types of functional composition (Fig. S4).

The association of functional composition with rising CO_2 levels largely mirrored that of the calendar year, due to their high correlation (r^2 = 0.99) (Figs. 6a, d). Similar to previous studies [3,15], increased CO_2 concentraiton was associated with deciduous broadleaved trees and higher drought tolerance across the study area (see black average lines in Figs. 6a, d). However, our new finding was that although the response slope of broadleaves vs conifers to rising CO_2 was consistent across the spatial gradient of baseline climate (Fig. 6a), the positive relationship between rising CO_2 levels and the functional shift toward drought tolerance (or shade intolerance) was more prominent in colder plots (the lower panel of Fig. 6d). This was attributable to the trends that rising CO_2 levels were also related to the reduced relative abundance of drought-intolerant *Picea* spp. (Table S2) and increased abundance of drought-tolerant/shade-intolerant *Pinus* spp. and early successional *Betula* spp. (Table S2) in colder plots (Fig. S5b). Although there was also a negative relationship between rising CO_2 levels and the relative abundance of *Picea* spp. in humid plots (Fig. S5a), their association was weaker. Thus it was not translated to ecologically meaningful trends in community-level functional shifts. Specifically, our study enhanced previous findings by showing that drought-tolerant and early-successional (resource acquisitive or fast-growing species [3,21]) might have benefitted more from rising CO_2 levels in colder plots, which was likely due to the extended growing season.

This might have augmented the growth of shade-intolerant (i.e., early successional) species in colder plots; however, in turn, it might have also facilitated mortality [42,43], leading to faster changes in composition toward drought tolerance/shade intolerance. In addition to rising CO_2, other environmental drivers, such as nitrogen deposition, might have also influenced functional shifts. However, in most parts of Canada, nitrogen deposition occurs at low levels [44], thus it is not very likely to drive significant changes in composition. Therefore, it is likely that rising CO_2 was at least partially responsible for the baseline

climate-dependent shifts in functional composition over the study period. Nevertheless, other factors may have also contributed to the observed functional shifts.

Across the study areas, warming and temporal changes in water availability had negligible effects on functional composition (Fig. S4; average effects are also shown as black lines in Figs. 6b, e). Temporal increases in temperature were associated with the higher relative abundance of drought intolerant *Abies* spp. and with decreased *Betula* spp. in humid plots (Fig. S5a), and with increased *Betula* spp. in warmer plots. However, warming had no association with both types of community-level functional composition regardless of the baseline climate. Our results contradicted a previous study, which showed that warming had positive effects on the growth of *Picea mariana*, particularly at higher latitudes (i.e., colder areas) in Eastern Canada [13]. This suggested that such trends may not be pervasive at larger scales across Canada, but rather regionally specific.

Temporal changes in water availability consistently had no relationship with both types of functional composition throughout the baseline climate gradient (Figs. 6c, f). Although a decrease in the relative abundance of *Picea* spp. (with the temporal reduction in water availability) was more prominent in historically drier plots (Fig. S5a), and an increase in the relative abundance of *Pinus* spp. was greater in colder plots (Fig. S5b), these changes were not translated to shifts in functional composition. Our result was consistent with a previous study of the boreal forests of Western Canada, as it also showed no significant influence of temporal variations in water availability to life history-based composition [15].

Previous studies in temperate and boreal forests at the regional scale revealed that the functional composition of forests shifted toward fast-growing and drought-tolerant identity (or early-successional and deciduous traits) with rising CO_2 levels, increasing temperatures, or decreased water availability [9,15,30]. However, we found clear patterns in functional composition as relates to the baseline climate: colder plots experienced more rapid functional shifts toward drought tolerance under rising CO_2 levels than in warmer plots. Moreover, we also found that the functional shifts toward deciduous broadleaved trees, as well as the regional trends observed in previous studies [29,34], were persistent and pervasive across biomes in North America. Thereby, our study generalized the findings from regional observations [3,4,7,9,15] to larger spatial networks across multiple biomes (i.e., boreal forest, temperate broadleaved and mixed forests, and temperate coniferous forests [45]) in North America.

While global environmental change is anticipated to intensify, our study suggests the vulnerability of the composition (higher rates in compositional changes from their original states [46]) of colder plots after experiencing, and as a result of, these environmental changes). As these compositional shifts are likely to impact the functioning of forest ecosystems (e.g., net changes in biomass through growth and mortality) [9] by altering their functional identity [47], our findings of baseline climate-dependent functional shifts may partially elucidate the spatial variations in the impacts of global environmental on forest ecosystem functions [13,14,16]. Since such macro-scale interactions remain largely elusive and need exploratory analysis, the applications of artificial intelligence can be helpful for pattern discovery [48,49].

These environmental change-induced functional shifts could have significant impacts on temperate and boreal forests. Specifically, greater increases in the capacity for resource acquisition (or early-successional functional identity) might consequently be translated to increased productivity and mortality [42,43,50], while increases in drought-tolerant abilities could result in reduced productivity and mortality in the face of changes brought about by global warming [9,50,51]. To ensure the sustainable functioning of forest ecosystems, future ecosystem management strategies should consider spatial differences in the response of forest composition to global environmental change, with a particular emphasis on colder forests experiencing higher rates of warming and compositional changes.

Methods

Study area and forest inventory data

To examine the temporal compositional shifts, we used a large network of permanent sampling plots (PSP), which were established by the provincial governments of British Columbia, Alberta, Saskatchewan, Manitoba, Ontario, Quebec, Nova Scotia, Newfoundland, and Labrador between the 1950's and 1980's (Fig. 1). We selected the PSPs that fit the following criteria. The plots must: (i) be unmanaged, with a known stand age (year); (ii) have all trees tagged and repeatedly measured; (iii) have all trees marked with their diameter at breast height (DBH). A total of 17,107 plots (914.21 ha; 43°47'N–60°00' N, 52°81'W–133°71' W) were selected for our analyses, with 1,438,577 trees measured during the monitoring period of from 1951 to 2016. The average measurement interval was 9.47 years with 4.70 census times, where the initial and final census years varied as 1951-2011 and 1956-2016, respectively. The plot sizes ranged from between 20 m^2 and 2,023 m^2 (Table S1). The mean annual temperature and precipitation in the area varied between -3.91 °C and 12.26 °C, and between 291 mm and 3,884 mm (1951-2016), respectively. The elevation ranged from 0.1 m to 2,355 m above sea level (Table S1).

Functional composition

To quantify functional composition, we employed eight key functional traits related to growth and competitive abilities, as well as environmental tolerance capacities, based on previous studies [18,20,21]: 'leaf nitrogen content per leaf dry mass' (N_{mass}, mg g^{-1}), 'leaf phosphorus content per leaf dry mass' (P_{mass}, mg g^{-1}), 'specific leaf area' (SLA, mm^2 mg^{-1}; i.e., leaf area per leaf dry mass), 'wood density' (WD, g cm^{-3}), 'shade tolerance' (ST, categorical class 1–5 [18]), 'drought tolerance' (DT, categorical class 1–5 [18], 'leaf habit' ('deciduous' = '1' *vs* 'evergreen' = '0'), and 'leaf structure' ('broadleaves' = '1' *vs* 'coniferous' = '0'). These trait values were extracted from the TRY database [22] and other published sources [18,23-26]. We obtained trait data for > 92% of all species. For those minor species of which trait data was absent, we used genus-level trait values (averaged for the genus) [27,28].

The functional composition was represented by the CWM [4,17,29] that weighs trait values according to the relative abundance of each species based on DBH [15]. Similar to previous studies [30], we performed a PCA

with the CWMs of the eight traits to obtain a comprehensive functional identity to represent them, as these values were highly correlated with each other (Fig. 2). We employed the first (CWM_{PC1}, explained 60% of the variation) and second axes (CWM_{PC2}, explained 22% of the variation) as proxies for functional composition. The CWM_{PC1} collectively represented traits associated with deciduous broadleaved trees and higher resource acquisition [18,21,23,24], being positively related with CWM_{Nmass}, CWM_{Pmass}, CWM_{SLA}, CWM_{Habit} (i.e., deciduous), CWM_{Struct} (i.e., broadleaves), and CWM_{WD}. On the contrary, the CWM_{PC2} represented traits associated with environmental tolerance, being negatively associated with CWM_{DT} and positively related with CWM_{ST} (Fig. 2).

Stand age

Stand age (SA) represents changes in stem density and composition associated with forest succession [15,19]) The SA of each plot was determined through dendrochronological aging based on the average age of the oldest species in the stand. We employed SA to account for the effects of forest development processes on functional composition.

Global environmental change drivers

Similar to previous studies [4,15], we used the calendar year (Year), which represented the effects of global environmental change overall on functional composition. For global environmental change drivers, we derived CO_2 measurements from the Mauna Loa Earth System Research Laboratory in Hawaii (http://www.esrl.noaa.gov/gmd/ccgg/trends/co2_data_mlo.html), and annual mean temperature, as well as annual mean precipitation and potential evapotranspiration, using *BioSIM* 11 software [31]. *BioSIM* generates plot-level climates, based on the simulation using daily observations and monthly historical statistics from the sampled points (latitude/longitude), being adjusted by differences in elevation. Therefore, the generated climate data was unique to each plot. Subsequently, we calculated the annual climate moisture index (CMI; mean annual precipitation minus potential evapotranspiration [32]). Following a previous study [15,19], we calculated the anomalies of annual mean temperature (ATA) and climate moisture index (ACMIA), which were defined as a deviation from their long-term means between 1951 and 2016 [33]. CMI is extensively employed as an indicator of drought conditions in Canada [15,19,32]. Negative values indicate drier conditions, while positive values denote wetter conditions.

Baseline climate

Following previous studies [13,14], we calculated the long-term averages between 1951 and 2016 of annual CMI (CMI_{ave}) and MAT (MAT_{ave}) for each plot, as proxies for site-specific baseline climates (i.e., local historical climate; Table S1; Fig. 1).

Statistical analysis

To examine the temporal trends of functional shifts associated with spatial variations in baseline climates, we employed the following linear mixed models:

$$(CWM_{PC1})_{ijkl} \text{ or } (CWM_{PC2})_{ijkl} = \beta_0 + \beta_1 \times (PS)_j + \beta_2 \times (Prov)_j + \beta_3 \times f(SA)_{ij} + \beta_4 \times (Year)_i +$$

$$\beta_5 \times (CMI_{ave})_j + \beta_6 \times (MAT_{ave})_j + \beta_7 \times f(SA)_{ij} \times (Year)_i +$$

$$\beta_8 \times f(SA)_{ij} \times (CMI_{ave})_j + \beta_9 \times f(SA)_{ij} \times (MAT_{ave})_j +$$

$$\beta_{10} \times (Year)_{ij} \times (CMI_{ave})_j + \beta_{11} \times (Year)_{ij} \times (MAT_{ave})_j +$$

$$\beta_{12} \times (CMI_{ave})_j \times (MAT_{ave})_j + \pi_j + \varepsilon \qquad (1)$$

where *i* and *j* are *i*th census and *j*th plot; CWM_{PC1} and CWM_{PC2} are community-weighted mean of 'broadleaves *vs* conifers traits' [30] and 'stress-tolerance traits' [18], respectively; β are the coefficients to be estimated; SA is the stand age being transformed by a square root function *f* based on Akaike Information Criterion (AIC); Year is the calendar year representing long-term global environmental change effects [15,19]. To control for potential influences of plot size on composition [34], we included plot size (PS) in the model as a covariate. We also inculded province (Prov) to account for differences in sampling methods (e.g., DBH threshold for tree measurement [35]) among provinces. The identities of each plot was included as a random effect (p_j) to take locally unique conditions (site-specific disturbance histories; e.g., short-term climate events, insect outbreaks, non-catastrophic small fire/wind/flooding disturbances) and spatial autocorrelation structures into account. ε was a random error. All of the two-way interaction terms were included, as the model that included these showed a consistently lower AIC according to our preliminary analysis. The maximum variance inflation factor (VIF) was 2.77 for the CWM_{PC1} model and 2.79 for the CWM_{PC2} model, indicating that multicollinearity was not an issue.

As the measurement interval (years) varied between censuses, we performed variation partitioning involving those fixed variables above and distance-based Moran's eigenvector maps (dbMEM) [36] to explicitly factor out the influences of temporal autocorrelation on functional composition. A dbMEM matrix was generated based on the calendar year as explanatory variables of temporaly correlated structures, using the *adespatial* package [37] in *R*. We initally selected 24 MEMs that well represented temporaly correlated structures, using Moran's *I* statistic with 1,000 random permutation [37]. We then selected nine dbMEMs for the CWM_{PC1} model and 11 dbMEMs for the CWM_{PC2} model by stepwise selection and added them to eqn. 1, as well as subsequent analyses with global environmental drivers (eqn. 2), as covariates to account for temporal autocorrelations [36]. After modelling with the dbMEMs, there was no significant temporal autocorrelation (examined by autocorrelation function estimation using the *acf* function in the *stats* package). Note that the coefficient estimates of the dbMEMs are shown separately for brevity since it is not our intension to understand the importance of autocorrelative structure (Fig. S6).

To account for uncertainties in sampling, models, and parameters we employed Bayesian Markov chain Monte Carlo methods for linear mixed models, using the *MCMCglmm* package [38]. To obtain a reliable posterior distribution with a satisfactorily effective sample size (i.e., the size of an uncorrelated sample), we used a thinning interval with a *lag* of 50 (examined by *autocorr.diag* function in the *MCMCglmm* package). Thus, we ran the models for 53,000 iterations with a burn-in period of 3,000 and thinning interval of 50 to achieve the recommended >1,000 effective sample size [39] (checked by *effectiveSize* function in the *MCMCglmm* package). We estimated the posterior distribution with a sampling of 1,000 in accordance with the default and confirmed that the performance stabilized with no autocorrelation [40]. All explanatory variables were centred and scaled (mean = 0, SD = 1) prior to analysis to allow a coefficient comparison.

We also examined the temporal trends in atmospheric CO_2 concentrations, ATA, and ACMIA, and how they were associated with the CMI_{ave} and MAT_{ave} via linear fixed effects models. To investigate the associations between the CWMs and rates of global environmental change, we replaced baseline climate variables (CMI_{ave} and MAT_{ave}) in eqn. 1 with temporal change rates in ACMIA ($ACMIA_{ChangeRate}$, cm/yr; Fig. 1c) and ATA ($ATA_{ChangeRate}$, °C/yr; Fig. 1d). Furthermore, we explored the roles of global environmental drivers on the CWMs using the following model (simultaneous modelling with three environmental change drivers rather than the Year term in eqn. 1):

$$(CWM_{PC1})_{ijkl} \text{ or } (CWM_{PC2})_{ijkl} = \beta_0 + \beta_1 \times (PS)_j + \beta_2 \times (Prov)_j + \beta_3 \times f(SA)_{ij} + \beta_4 \times (CO_2)_i +$$

$$\beta_5 \times (ATA)_i + \beta_6 \times (ACMIA)_i + b_7 \times (CMI_{ave})_j + \beta_8 \times (MAT_{ave})_j +$$

$$\beta_9 \times f(SA)_{ij} \times (CO_2)_i + \beta_{10} \times f(SA)_{ij} \times (ATA)_{ij} +$$

$$\beta_{11} \times f(SA)_{ij} \times (ACMIA)_{ij} + \beta_{12} \times f(SA)_{ij} \times (CMI_{ave})_j +$$

$$\beta_{13} \times f(SA)_{ij} \times (MAT_{ave})_j + \beta_{14} \times (CO_2)_i \times f(CMI_{ave})_j +$$

$$\beta_{15} \times f(ATA)_{ij} \times (CMI_{ave})_j + \beta_{16} \times f(ACMIA)_{ij} \times (CMI_{ave})_j +$$

$$\beta_{17} \times (CO_2)_i \times f(MAT_{ave})_j + \beta_{18} \times f(ATA)_{ij} \times (MAT_{ave})_j +$$

$$\beta_{19} \times f(ACMIA)_{ij} \times (MAT_{ave})_j + \beta_{20} \times f(CMI_{ave})_j \times (MAT_{ave})_j +$$

$$\pi_j + \varepsilon \qquad (2)$$

where CO_2, ATA, and ACMIA are the atmospheric CO_2 concentration, anomalies of mean annual temperature, and climate moisture index, with which the CO_2 and ATA in our data was positively correlated ($r^2 = 0.19$). As the maximum VIF in this model was = 4.33 for the CWM_{PC1} model and 4.34 for the CWM_{PC2} model, concerning the multicollinearity, we also modelled CWMs with each of the climate drivers separately (one driver at a time). This preliminary attempt showed that the coefficient estimates

did not qualitatively differed among these models and eqn. 2 (Fig. S4). Therefore, similar to a previous study [19], we focused on the outcomes from the simultaneous model with eqn.2. Conditional and marginal R^2 for eqns. 1 and 2 are shown in Table S3.

To understand the functional response processes to the calendar year, and global environmental change drivers, we calculated genus-level relative abundance (%) by sub-setting the basal area (m^2/ha) by major tree genus. Similar to a previous study [19], major tree genus was defined as those that accounted for >5% of the total basal area across all of the plots during the entire census, and occurred in all the provinces: *Picea* spp. (26.7%); *Abies* spp. (11.8%); *Populus* spp. (8.5%); *Acer* spp. (7.9%); and *Pinus* spp. (15.4%) (Table S2). The basal areas of individual stems were summed to obtain the overall basal area. The relative abundance of each major genus was calculated as the proportion of its basal area to the total basal area of the stand at each census for each plot, which was then multiplied by 100 to obtain an abundance percentage [15]. Similar to a previous study [15], we then examined the responses of the relative abundance of each genus to the calendar year, with the same fixed-effects parameters used in eqn. 1, as well as the three global environmental change drivers with the same fixed effects used in eqn. 2.

For the interpretation of all analyses, we focused on not the statistical significance (i.e., p-value) but the 'ecological significance'; that is, the effect sizes and the directionality and steepness of slopes (positive/negative/neutral directionalities). If these elements were substantially different, we interpreted as an ecologically meaningful trend in functional shifts, while we considered statistically significant but small effect sizes that result in qualitatively similar slopes as negligible difference. Although such evaluation scheme cannot offer an exact threshold for conclusion in comparison to statistical significance level, we advocate that statistical significance does not necessarily equal to ecological significance, and statistical assessment based on effect size should be the standard, according to the recent statement by the American Statistical Association [41].

Declarations

Acknowledgements

We are grateful to Dr. Eric B. Searle for his assistance in data compilation. We also thank Dr. John Markham for his helpful comments on the manuscript. We appreciate the Provincial Governments of British Columbia, Alberta, Saskatchewan, Manitoba, Ontario, Quebec, Nova Scotia, and Newfoundland, and Labrador for providing detailed data. We also thank the TRY initiative for providing the plant traits database (http://www.try-db.org). This study was supported by the Natural Sciences and Engineering Research Council of Canada (RGPIN-2014-0418 and STPGP 506284). M.H. and X.C. thank the Government of Ontario for the Ontario Trillium Scholarship. M.H. was also supported by Japan Society for the Promotion of Science (JSPS) KAKENHI: grant number 20J00178.

Author contributions

M.H. and H.Y.H.C. conceived the study; M.H. analysed the data with significant contributions from M.R. and H.Y.H.C.; M.H. led the writing of the initial draft, and all authors contributed to writing the final manuscript.

Competing interests: Authors declare no competing interests.

Data availability: Authors confirm that the data and *R* codes supporting the results will be archived in an appropriate public repository.

References

1. Dornelas, M. *et al.* Assemblage Time Series Reveal Biodiversity Change but Not Systematic Loss. *Science* **344**, 296–299, doi:10.1126/science.1248484 (2014).
2. Ryo, M., Aguilar-Trigueros, C. A., Pinek, L., Muller, L. A. H. & Rillig, M. C. Basic Principles of Temporal Dynamics. *Trends in Ecology & Evolution* **34**, 723–733, doi:https://doi.org/10.1016/j.tree.2019.03.007 (2019).
3. Laurance, W. F. *et al.* Pervasive alteration of tree communities in undisturbed Amazonian forests. *Nature* **428**, 171–175, doi:10.1038/nature02383 (2004).
4. Esquivel-Muelbert, A. *et al.* Compositional response of Amazon forests to climate change. *Global Change Biology* **25**, 39–56, doi:10.1111/gcb.14413 (2019).
5. Fadrique, B. *et al.* Widespread but heterogeneous responses of Andean forests to climate change. *Nature* **564**, 207–212, doi:10.1038/s41586-018-0715-9 (2018).
6. Bjorkman, A. D. *et al.* Plant functional trait change across a warming tundra biome. *Nature* **562**, 57–62, doi:10.1038/s41586-018-0563-7 (2018).
7. Aguirre-Gutiérrez, J. *et al.* Drier tropical forests are susceptible to functional changes in response to a long-term drought. *Ecology Letters* **22**, 855–865, doi:10.1111/ele.13243 (2019).
8. Bartlett, M. K., Detto, M. & Pacala, S. W. Predicting shifts in the functional composition of tropical forests under increased drought and CO2 from trade-offs among plant hydraulic traits. **22**, 67–77, doi:10.1111/ele.13168 (2019).
9. Zhang, T., Niinemets, U., Sheffield, J. & Lichstein, J. W. Shifts in tree functional composition amplify the response of forest biomass to climate. *Nature* **556**, 99–102, doi:10.1038/nature26152 (2018).
10. Hisano, M., Searle, E. B. & Chen, H. Y. H. Biodiversity as a solution to mitigate climate change impacts on the functioning of forest ecosystems. *Biological Reviews* **93**, 439–456, doi:10.1111/brv.12351 (2018).
11. Isbell, F. *et al.* Linking the influence and dependence of people on biodiversity across scales. *Nature* **546**, 65–72, doi:10.1038/nature22899 (2017).
12. Overpeck, J. T. & Conde, C. A call to climate action. *Science* **364**, 807, doi:10.1126/science.aay1525 (2019).

13. D'Orangeville, L. *et al.* Northeastern North America as a potential refugium for boreal forests in a warming climate. *Science* **352**, 1452–1455, doi:10.1126/science.aaf4951 (2016).
14. Luo, Y., Chen, H. Y. H., McIntire, E. J. B., Andison, D. W. & Gilliam, F. Divergent temporal trends of net biomass change in western Canadian boreal forests. *Journal of Ecology* **107**, 69–78, doi:10.1111/1365-2745.13033 (2019).
15. Searle, E. B. & Chen, H. Y. H. Persistent and pervasive compositional shifts of western boreal forest plots in Canada. *Global Change Biology* **23**, 857–866, doi:10.1111/gcb.13420 (2017).
16. Huang, M. *et al.* Velocity of change in vegetation productivity over northern high latitudes. *Nat Ecol Evol* **1**, 1649–1654, doi:10.1038/s41559-017-0328-y (2017).
17. Lavorel, S. *et al.* Assessing functional diversity in the field – methodology matters! *Functional Ecology* **22**, 134–147, doi:10.1111/j.1365-2435.2007.01339.x (2008).
18. Niinemets, U. & Valladares, F. Tolerance to shade, drought, and waterlogging of temperate Northern Hemisphere trees and shrubs. *Ecological Monographs* **76**, 521–547, doi:10.1890/0012-9615(2006)076[0521:Ttsdaw]2.0.Co;2 (2006).
19. Hisano, M., Chen, H. Y. H., Searle, E. B. & Reich, P. B. Species-rich boreal forests grew more and suffered less mortality than species-poor forests under the environmental change of the past half-century. *Ecology Letters* **22**, 999–1008, doi:10.1111/ele.13259 (2019).
20. Anderegg, W. R. L. *et al.* Hydraulic diversity of forests regulates ecosystem resilience during drought. *Nature* **561**, 538–541, doi:10.1038/s41586-018-0539-7 (2018).
21. Reich, P. B. The world-wide 'fast-slow' plant economics spectrum: a traits manifesto. *Journal of Ecology* **102**, 275–301, doi:Doi 10.1111/1365-2745.12211 (2014).
22. Kattge, J. *et al.* TRY - a global database of plant traits. *Global Change Biology* **17**, 2905–2935, doi:10.1111/j.1365-2486.2011.02451.x (2011).
23. Wright *et al.* The worldwide leaf economics spectrum. *Nature* **428**, 821–827, doi:10.1038/nature02403 (2004).
24. Chave, J. *et al.* Towards a worldwide wood economics spectrum. *Ecol Lett* **12**, 351–366, doi:10.1111/j.1461-0248.2009.01285.x (2009).
25. Berner, L. T. & Law, B. E. Plant traits, productivity, biomass and soil properties from forest sites in the Pacific Northwest, 1999–2014. *Scientific Data* **3**, 160002, doi:doi:10.1038/sdata.2016.2 (2016).
26. Reich & Oleksyn, J. Global patterns of plant leaf N and P in relation to temperature and latitude. *Proceedings of the National Academy of Sciences of the United States of America* **101**, 11001–11006, doi:10.1073/pnas.0403588101 (2004).
27. Swenson, N. G. & Enquist, B. J. Ecological and evolutionary determinants of a key plant functional trait: wood density and its community-wide variation across latitude and elevation. *American Journal of Botany* **94**, 451–459, doi:10.3732/ajb.94.3.451 (2007).
28. Carreño-Rocabado, G. *et al.* Effects of disturbance intensity on species and functional diversity in a tropical forest. *Journal of Ecology* **100**, 1453–1463, doi:10.1111/j.1365-2745.2012.02015.x (2012).

29. Ruiz-Benito, P. *et al.* Functional diversity underlies demographic responses to environmental variation in European forests. *Global Ecol Biogeogr* **26**, 128–141, doi:10.1111/geb.12515 (2017).
30. Ruiz-Benito, P. *et al.* Climate- and successional-related changes in functional composition of European forests are strongly driven by tree mortality. *Global Change Biology* **23**, 4162–4176, doi:10.1111/gcb.13728 (2017).
31. Régnière, J., St-Amant, R. & Béchard, A. *BioSIM 10–User's manual*. (2014).
32. Hogg, E. H., Michaelian, M., Hook, T. I. & Undershultz, M. E. Recent climatic drying leads to age-independent growth reductions of white spruce stands in western Canada. *Glob Chang Biol* **23**, 5297–5308, doi:10.1111/gcb.13795 (2017).
33. Clark, J. S., Bell, D. M., Hersh, M. H. & Nichols, L. Climate change vulnerability of forest biodiversity: climate and competition tracking of demographic rates. *Global Change Biology* **17**, 1834–1849, doi:10.1111/j.1365-2486.2010.02380.x (2011).
34. Searle, E. B. & Chen, H. Y. H. Climate change-associated trends in biomass dynamics are consistent across soil drainage classes in western boreal forests of Canada. *For Ecosyst* **4**, 1–11, doi:ARTN 1810.1186/s40663-017-0106-y (2017).
35. Searle, E. B. & Chen, H. Y. H. Tree size thresholds produce biased estimates of forest biomass dynamics. *Forest Ecol Manag* **400**, 468–474, doi:10.1016/j.foreco.2017.06.042 (2017).
36. Legendre, P. & Gauthier, O. Statistical methods for temporal and space-time analysis of community composition data. *Proceedings of the Royal Society B: Biological Sciences* **281**, 20132728, doi:10.1098/rspb.2013.2728 (2014).
37. Dray, S. *et al.* Package 'adespatial'. *R package version* **ver**. **0.3-8**, Available at: https://cran.microsoft.com/web/packages/adespatial/adespatial.pdf (2020).
38. Hadfield, J., Hadfield, M. J. & SystemRequirements, C. Package 'MCMCglmm'. *R package version* **ver**. **2.29**, Available at: http://cran.ms.unimelb.edu.au/web/packages/MCMCglmm/MCMCglmm.pdf (2019).
39. de Villemereuil, P. Estimation of a biological trait heritability using the animal model. *How to use the MCMCglmm R package*, 1–36 (2012).
40. Ryo, M., Yoshimura, C. & Iwasaki, Y. Importance of antecedent environmental conditions in modeling species distributions. *Ecography* **41**, 825–836, doi:10.1111/ecog.02925 (2018).
41. Wasserstein, R. L., Schirm, A. L. & Lazar, N. A. Moving to a World Beyond "p < 0.05". *The American Statistician* **73**, 1–19, doi:10.1080/00031305.2019.1583913 (2019).
42. Searle, E. B. & Chen, H. Y. H. Temporal declines in tree longevity associated with faster lifetime growth rates in boreal forests. *Environ Res Lett* **13**, 125003, doi:ARTN 1250031088/1748–9326/aaea9e (2018).
43. Brienen, R. J. *et al.* Long-term decline of the Amazon carbon sink. *Nature* **519**, 344–348, doi:10.1038/nature14283 (2015).

44. Reay, D. S., Dentener, F., Smith, P., Grace, J. & Feely, R. A. Global nitrogen deposition and carbon sinks. *Nature Geoscience* **1**, 430–437, doi:10.1038/ngeo230 (2008).
45. Olson, D. M. *et al.* Terrestrial Ecoregions of the World: A New Map of Life on Earth: A new global map of terrestrial ecoregions provides an innovative tool for conserving biodiversity. *BioScience* **51**, 933–938, doi:10.1641/0006-3568(2001)051[0933:TEOTWA]2.0.CO;2 %J BioScience (2001).
46. MacDonald, R. L., Chen, H. Y. H., Bartels, S. F., Palik, B. J. & Prepas, E. E. Compositional stability of boreal understorey vegetation after overstorey harvesting across a riparian ecotone. *Journal of Vegetation Science* **26**, 733–741, doi:10.1111/jvs.12272 (2015).
47. Grime, J. P. Benefits of plant diversity to ecosystems: immediate, filter and founder effects. *Journal of Ecology* **86**, 902–910, doi:DOI 10.1046/j.1365-2745.1998.00306.x (1998).
48. Ryo, M. *et al.* Explainable Artificial Intelligence enhances the ecological interpretability of black-box species distribution models. *EcoEvoRxiv*, doi:doi:10.32942/osf.io/w96pk (2020).
49. Ryo, M. & Rillig, M. C. Statistically reinforced machine learning for nonlinear patterns and variable interactions. *Ecosphere* **8**, e01976, doi:10.1002/ecs2.1976 (2017).
50. Chen, H. Y. H. & Luo, Y. Net aboveground biomass declines of four major forest types with forest ageing and climate change in western Canada's boreal forests. *Global Change Biology* **21**, 3675–3684, doi:10.1111/gcb.12994 (2015).
51. Greenwood, S. *et al.* Tree mortality across biomes is promoted by drought intensity, lower wood density and higher specific leaf area. *Ecology letters* **20**, 539–553 (2017).

Figures

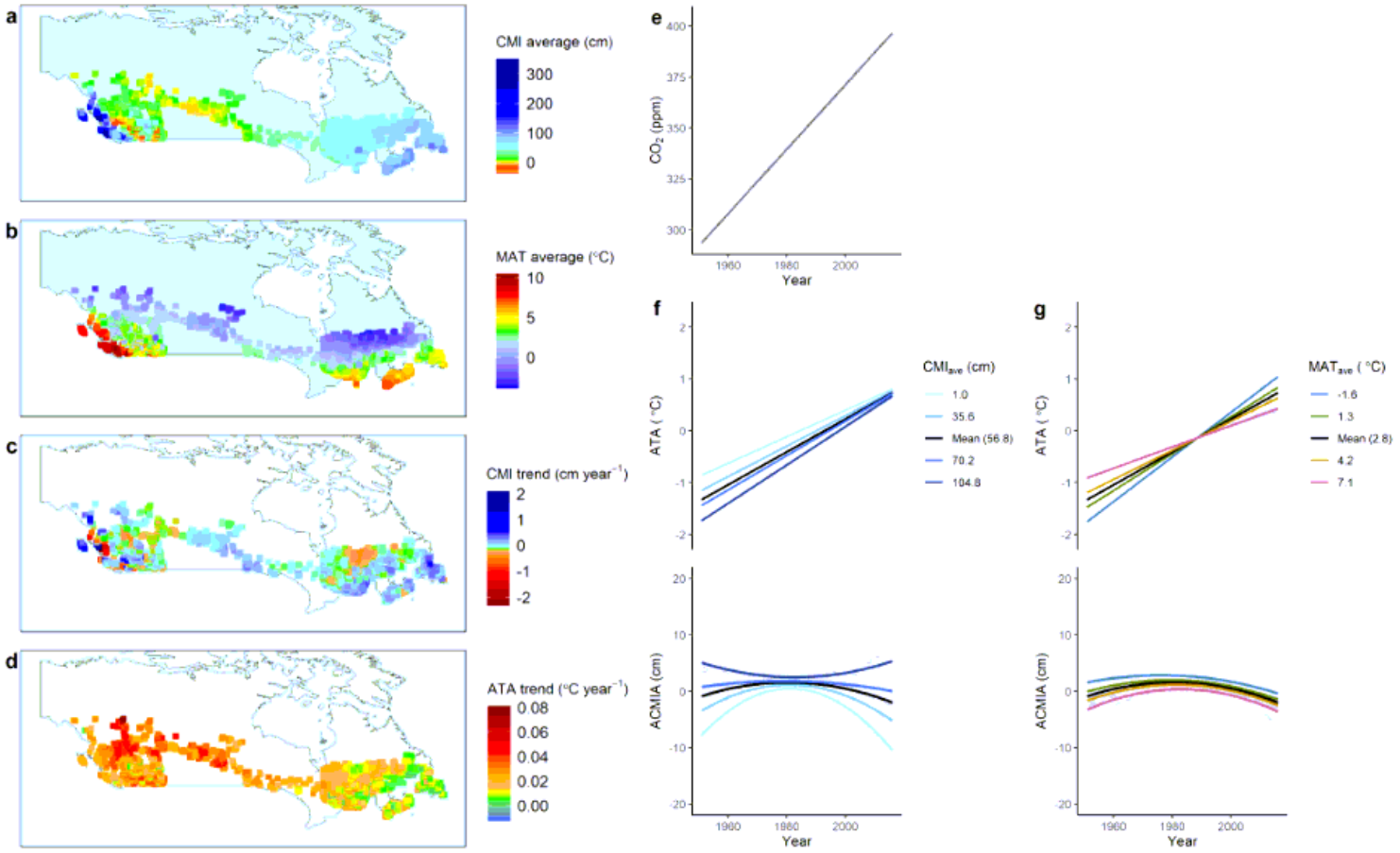

Figure 1

Permanent sampling plot locations across Canada, and spatiotemporal patterns of global environmental change drivers. Spatial climate is defined as long-term averages of the climate moisture index (CMIave, a) and mean annual temperature (MATave, b) between 1951 and 2016. Temporal trends of anomalies of annual CMI (ACMIA, c) and MAT (ATA, d) between 1951 and 2016. (e) Temporal trends in atmospheric CO2 concentrations. ATA and ACMIA (temporal trends in climate) in relation to the long-term averages of climate moisture index (CMIave, f) and mean annual temperature (MATave, g) (spatial variations in baseline climate) with ranges of their 5th and 95th percentiles. Grey dots and error bars show yearly mean (temporal trends in climate) and their 95% confidence intervals. Lines are mean values of the temraporal trends in ATA and ACMIA with their 95% confidence intervals.

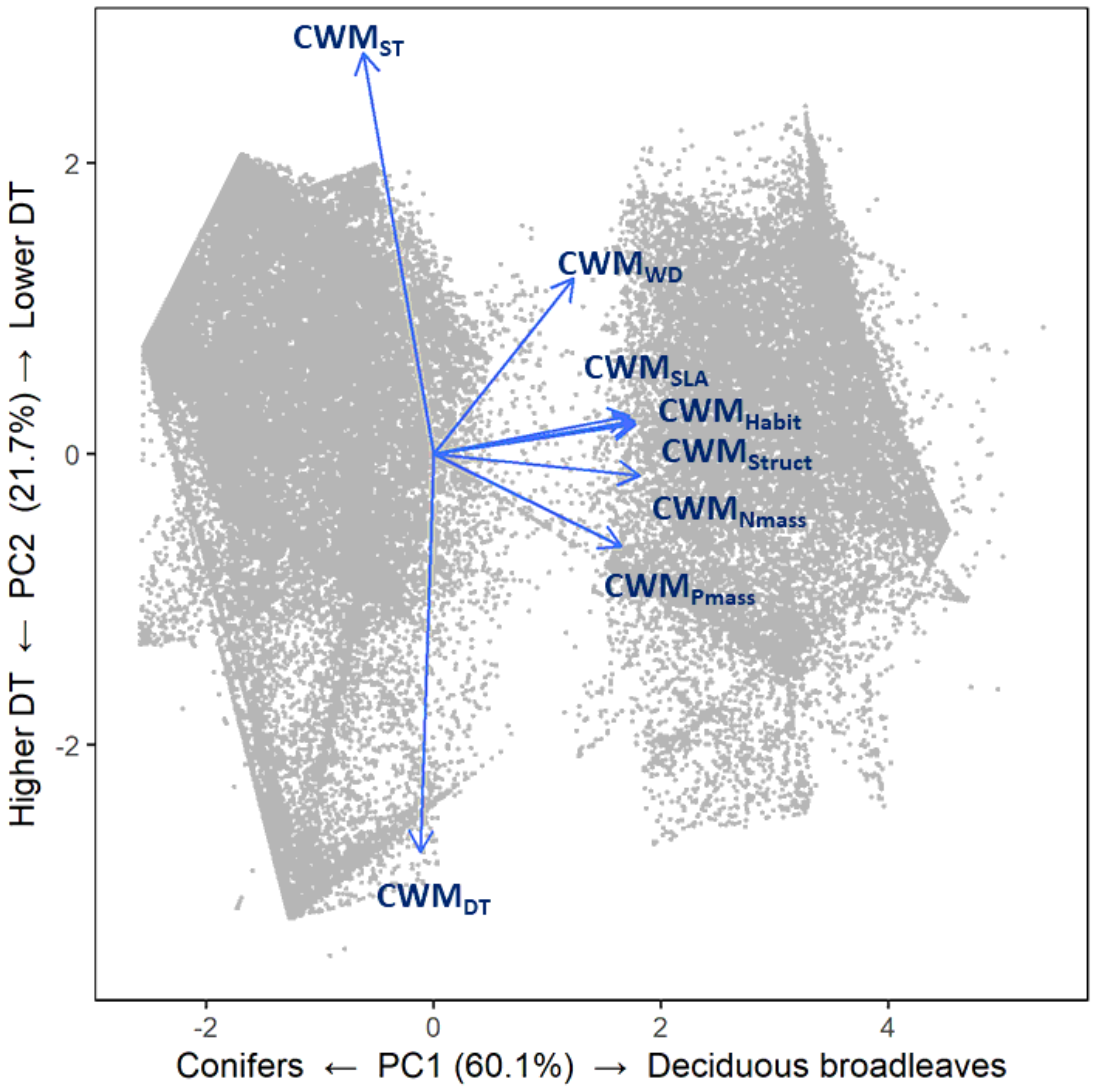

Figure 2

Results of principal component analysis (PCA) showing permanent sampling plots and each functional identity (community-weighted mean of trait value, CWM). CWMNmass = CWM of nitrogen content per leaf mass, CWMPmass = CWM of phosphorus content per leaf mass, CWMSLA = CWM of specific leaf area, CWMStruct = CWM of leaf structure, CWMHabit = CWM of leaf habit, CWMWD = CWM of wood density, CWMST = CWM of shade tolerance, CWMDT = CWM of drought tolerance. The first axis (PC1) represents traits associated with deciduous broadleaved trees vs conifers, while the second axis (PC2) refers to traits associated with environmental tolerance.

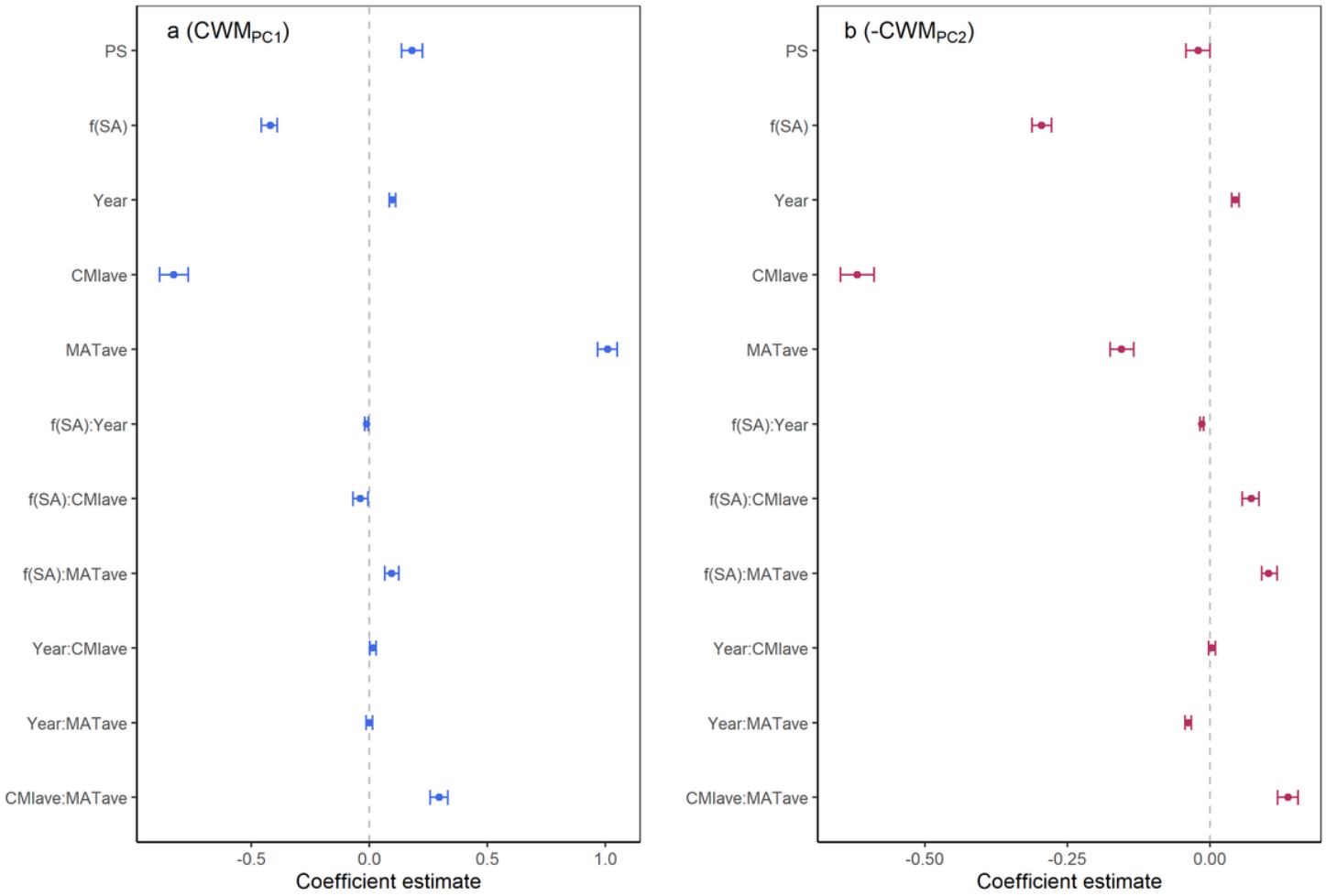

Figure 3

Fixed effects of stand age (SA, transformed by a squared root function f based on AIC), calendar year (Year), long-term averages of climate moisture index (CMIave), and mean annual temperature (MATave) on the community-weighted mean of trait values. Circles and error bars are means and 95% Bayesian confidence intervals. Higher CWMPC1 values indicate traits associated with deciduous broadleaved trees, while lower values indicate conifers (a, see Fig. 2). Higher CWMPC2 values (being multiplied by -1 to facilitate interpretation) indicates traits associated with higher drought tolerance (b, see Fig. 2). Fixed effects were scaled to allow a comparison of the strength of each effect to the response variable. Coefficient estimates of distance-based Moran's eigenvector maps for the simultaneous models are shown separately for convenience (Figs. S7a, b).

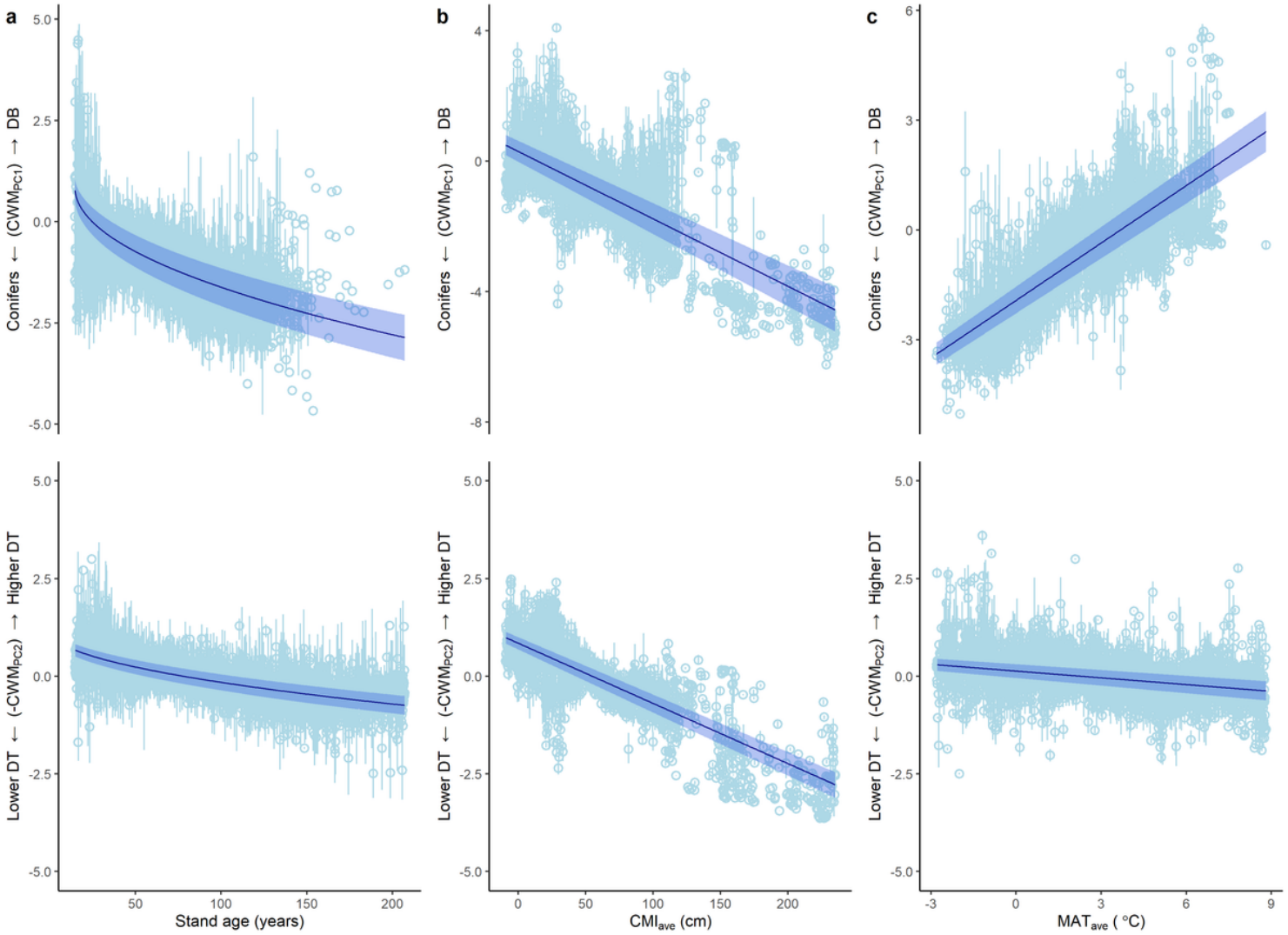

Figure 4

Temporal and spatial trends in functional composition. The main effects of stand age (a), the long-term average of climate moisture index (CMIave, b), and the long-term average of mean annual temperature (MATave, c) on community-weighted mean of trait values (CWMPC1 and -CWMPC2). CWMPC1 is a functional composition associated with deciduous broadleaved trees (higher value) vs conifers (lower value), while CWMPC2 is related to environmental tolerance (higher value = higher drought tolerance (DT); see Methods). Dots and error bars reflect the means and their 95% Bayesian confidence intervals. Blue lines are fitted main effects with their 95% Bayesian confidence intervals shown as shaded areas. Based on AIC, stand age was transformed by the squared root.

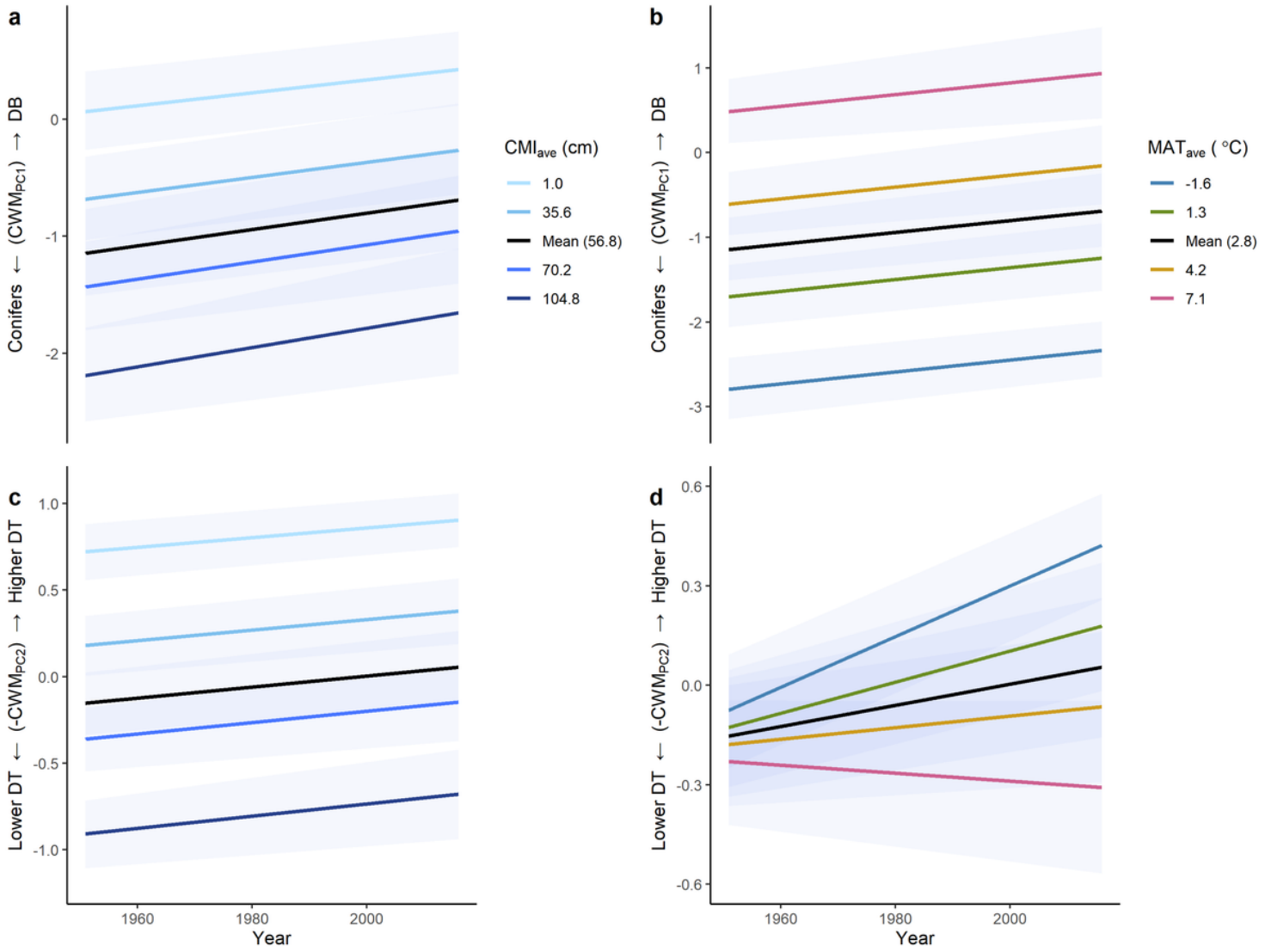

Figure 5

Temporal trends in community weighted-mean of traits associated with deciduous broadleaved trees vs conifers (CWMPC1) and drought tolerance (-CWMPC2). Trends dependent on the long-term averages of the climate moisture index (CMIave, a) and mean annual temperature (MATave, b). Values are means and their 95% Bayesian confidence intervals. CMIave and MATave were binned from 1.0 to 104.8 (cm) and from -1.6 to 7.1 (°C) (their 5th and 95th percentiles) for four levels.

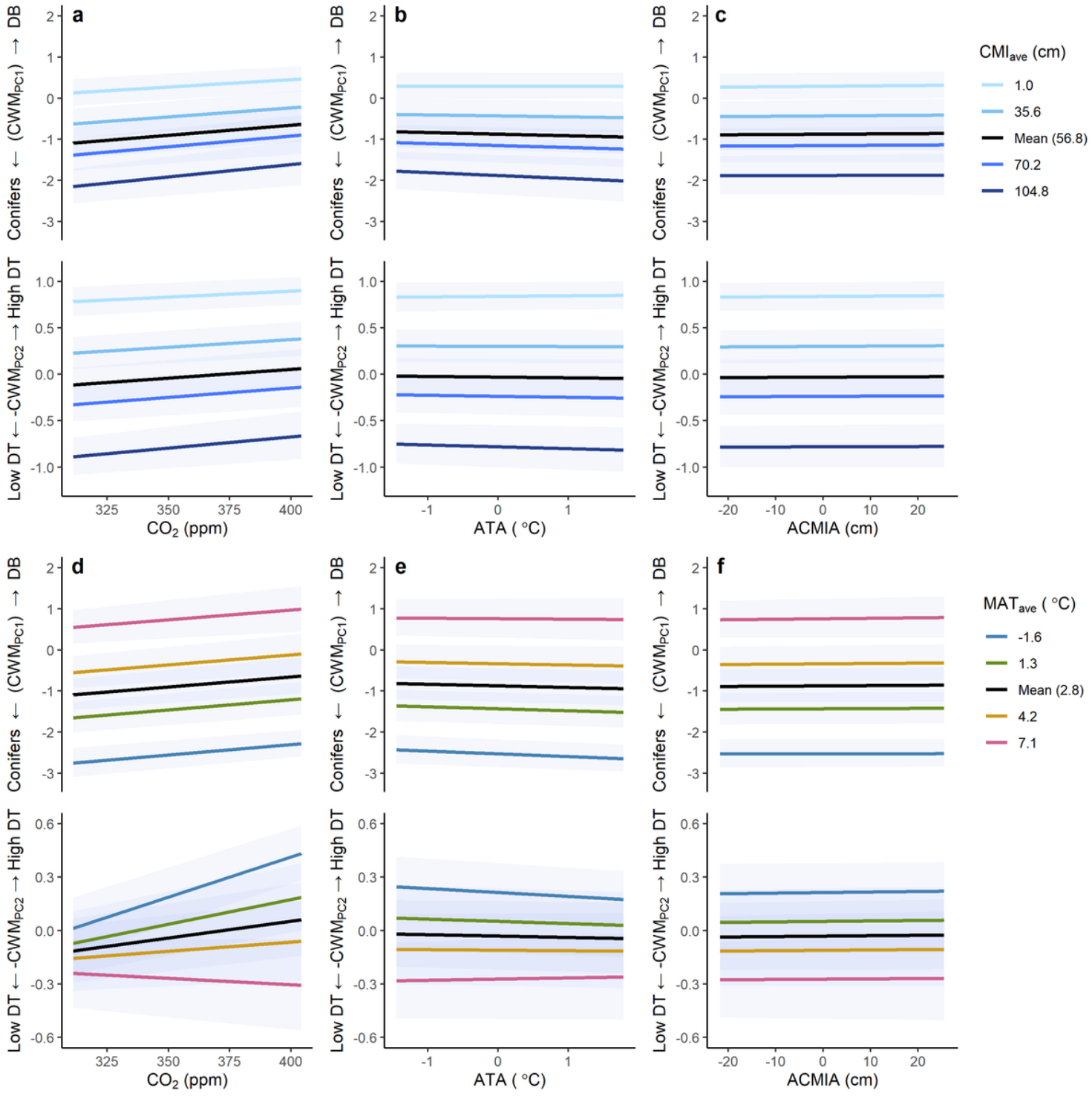

Figure 6

Responses of community weighted-mean of traits associated with deciduous broadleaved trees vs conifers (CWMPC1) and drought tolerance (DT, -CWMPC2¬) to global environmental change drivers [atmospheric CO2 concentration, anomaly of mean annual temperature (ATA), and anomaly of climate moisture index (ACMIA)]. Response slopes in relation to the long-term averages of climate moisture index (CMIave, a, b, c) and mean annual temperature (MATave, d, e, f) (shown as their 5th and 95th percentiles).

Values are means and their 95% Bayesian confidence intervals. CMIave and MATave were binned from 1.0 to 104.8 (cm) and from -1.6 to 7.1 (°C) (their 5th and 95th percentiles) for four levels.

Supplementary Files

This is a list of supplementary files associated with this preprint. Click to download.

- HisanoSupplementaryInformationNatCommun.docx